ACS OMEGA

Open Access

http://pubs.acs.org/journal/acsodf

Article

Robustly Adherable Hierarchical Nanostructures via Self-Bonding and Self-Texturing of Aluminum Nitride for Applications in Highly Efficient Oil/Water Separation

Handong Cho,* Jihoon Chung, and Sangmin Lee

Cite This: *ACS Omega* 2023, 8, 42732−42740

Read Online

ACCESS | Metrics & More | Article Recommendations

ABSTRACT: The release of wastewater containing oily contaminants into water bodies and soils severely threatens the environment and human health. Although several conventional techniques are used in treating oil/water mixtures and emulsions, these methods are often expensive, time-consuming, and inefficient. Porous membranes or sponges are widely used in filtration or absorption, but their use is limited by their low separation efficiencies and secondary contamination. Recently, a novel technology that is designed to selectively separate oil from oil/water mixtures or emulsions by using materials with special wetting surfaces was developed. Superwetting surfaces may be used to selectively separate oils from emulsions. This approach enables the use of materials with relatively large pores, resulting in high throughput properties and efficiencies. In this study, a facile method is proposed for use in preparing a superhydrophobic−superoleophilic felt fabric for utilization in separating oil/water mixtures and emulsions. By hydrolyzing aluminum nitride nanopowders, the desired micro-/nanostructures may be successfully fabricated and firmly attached to a fabric surface without using a binder resin. This results in various materials with special wetting properties, regardless of their sizes and shapes and the successful separation of oil and water from oil/water mixtures and emulsions in harsh environments. This approach exhibits promise as a low-cost, scalable, and efficient method of separating oily wastewater, with the potential for use in wider industrial applications.

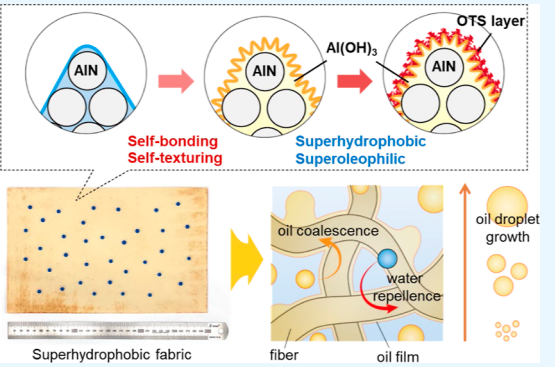

1. INTRODUCTION

Numerous wastewaters containing oily contaminants, which may occur as a result of various industrial processes, such as petroleum refining and metal manufacturing, are released into water bodies and soil and threaten not only humans but also the entire ecosystem.[1−3] Oily industrial wastewater can be categorized into two types: immiscible mixtures of oil and water and emulsions containing oil droplets as small as 20 μm in size, with the latter generally more challenging to separate.[4,5] Although several conventional techniques are reported for use in treating oil/water mixtures and emulsions, including physical separation using gravity and centrifugation,[6,7] chemical emulsion breaking using flocculants,[8,9] and biological treatment using microorganisms,[10,11] these approaches exhibit limitations such as high treatment costs, time-consuming processes, low separation efficiencies, and the formation of secondary pollutants.[12,13] Among the conventional oily wastewater treatment techniques, filtration or absorption methods utilizing porous membranes or sponges are traditionally widely used in industry, but they display the disadvantages of low separation efficiency and applicability only to the treatment of immiscible wastewater. In the case of filtration, in particular, the separation efficiency and throughput exhibit a trade-off relationship depending on the pore size of the filtering materials. When a membrane with large pores is used to increase throughput, the separation efficiency decreases and vice versa. In addition, as membranes may be easily fouled or clogged with oil during separation, the membrane should be periodically replaced to maintain separation performance, resulting in adverse environmental effects.[14] However, in adsorption using a polymeric sponge, the throughput is limited according to the oil-holding capacity of the material, and the material is utilized as landfill or incinerated after use, which may also cause secondary environmental pollution.[15] Therefore, extensive efforts have focused on efficiently and rapidly separating oil from water, along with overcoming these disadvantages.

Recently, a novel technology that may be used to selectively filter oil from oily wastewater by using materials with special

Received: July 28, 2023
Revised: October 14, 2023
Accepted: October 16, 2023
Published: October 31, 2023

https://doi.org/10.1021/acsomega.3c05524
ACS Omega 2023, 8, 42732−42740

wetting surfaces emerged. Surfaces with superwetting properties display opposing affinities for oil and water, and this property may be exploited to selectively separate oil/water mixtures,[16] e.g., a superhydrophobic surface exhibiting a high water contact angle over 150° may be completely wetted with oil, enabling the oil to permeate the (superhydrophobic−superoleophilic) membrane. Li et al. developed new biomimetic oleophilic conical structures.[17] Based on Laplace pressure and gradient wettability, the fabricated material efficiently collects oil droplets and sustains a high separation efficiency and throughput capacity. Woo et al. fabricated hierarchical microcubic and nanoflake structured surfaces with superhydrophobic/-hydrophilic pattern.[18] The patterned surface effectively captured and aggregated tiny oil droplets until they grew into sufficient size, demonstrating the separation of the oil/water emulsion with high efficiency. Compared to the traditional method, this approach enables the use of materials with relatively large pores, and thus, it exhibits the capacity to separate materials with high throughput and efficiency. The membrane is also green because it may be easily used after washing due to its excellent fouling resistance. These superhydrophobic−superoleophilic surfaces are typically realized via the integration of two critical components: hierarchical surface structures at the micro-/nanoscale and low-surface-energy materials. Two methods of fabricating materials for use in separating oily emulsions are well-known: (1) the direct fabrication of a porous material with micronano pores via the electrospinning of a hydrophobic polymer material[19,20] and (2) the formation of a structure at the micronano scale on a smooth porous material, which is then coated with a low-surface-energy material.[21,22] The former method may be used to design nanofibrous membranes with controllable pore sizes, which may separate oily emulsions with high efficiencies and large fluxes. However, their practical applications remain limited owing to their size-limited fabrication processes and inadequate mechanical strengths.[23] The latter method is simple and has the potential for application across diverse substrates, regardless of size and material, but the adhesion between the micronano materials on the surface and the underlying substrate often depends on weak electrostatic interactions, which results in a weak adhesion strength, and the surface structures may be easily damaged and delaminated under mechanical action.[24,25] Hence, it is necessary to develop a facile, cost-effective, and scalable approach of fabricating superhydrophobic−superoleophilic materials that can maintain surface structure and separation efficiency based on strong bonding between nanoparticles and substrates.

In this research, we introduce a straight-forward method of preparing micro/nano hierarchical structures on felt fabrics, without the use of any binders, by exploiting the self-adhesive properties and morphological evolution of aluminum nitride (AlN) nanopowders. To ensure a robust chemical bond between the AlN layer and the fabric, we propose a process of depositing AlN nanoparticles on plasma-treated fabrics, followed by applying a temporary protective coating to prevent detachment of AlN from the fabric surface during the hydrolysis reaction. Our approach allows for the formation of thin coating layers with special wetting properties that firmly adhere to the substrate, offering potential applications in various industries such as the oil/water mixture and emulsion separation. We also characterized the surface morphologies, chemical properties, and bonding of the AlN nanostructures deposited on the substrate. Moreover, we designed a simple device for emulsion separation and demonstrated its efficiency in treating emulsified oily wastewater in harsh environments.

2. MATERIAL AND METHODS

2.1. Materials. AlN nanopowders (99.5%) with a size of approximately 65−75 nm and hexagonal crystals were purchased from US Research Nanomaterials (Houston, TX, USA) and employed without further purification or alteration, and anhydrous ethanol (99.5%) and *n*-hexane (95%) were obtained from Duksan Pure Chemicals (Ansan, Republic of Korea). Soybean oil, *n*-octadecyltrichlorosilane (OTS), and Oil Red O were supplied by Thermo Fisher Scientific (Waltham, MA, USA), and diesel and gasoline were purchased from local gas stations. Nonwoven acrylic felt fabric sheets were used to achieve the superhydrophobic−superoleophilic surfaces.

2.2. Preparation of the Superhydrophobic−Superoleophilic Felt Fabric. Commercial acrylic felt fabric was cut into the desired shape and rinsed with water and ethanol to eliminate the impurities prior to use. A certain amount of AlN nanopowder (2 mg mL^{-1}) was added to ethanol, and the mixture was ultrasonicated to break up the clustered powder and disperse it more uniformly in the solution using an ultrasonic homogenizer (100 W, VCX 500, Sonics and Materials, Newtown, CT, USA). After treating a piece of fabric with oxygen plasma for 3 min at 100W using a low-frequency plasma generator (COVANCE-RF, Femto-Science, Republic of Korea), the fabric sample was then immersed in the aqueous solution and squeezed gently by hand to remove the excess solution. This dipping-squeezing process was repeated three times in total to yield a fabric surface coated evenly with AlN. The fabric was gently lifted out of the solution, and the wet surface was then dried at 65 °C to remove the solvent. Subsequently, the fabric was immersed in boiling water for 10 min, washed several times with deionized water, and dried thoroughly to completely remove any remaining water. This process was repeated three times to ensure that the nanostructures formed evenly on the fabric surface. Finally, to render the fabric surface superhydrophobic, it was soaked in hexane containing 0.1% (v/v) v/v of OTS for 10 min, rinsed with hexane, and dried in an oven at 65 °C for 12 h.

2.3. Characterizations. The surface morphology and composition were, respectively, characterized using field-emission scanning electron microscopy (SEM, Regulus8230, Hitachi, Tokyo, Japan) and energy-dispersive X-ray spectroscopy (EDS, Ultim Extreme, Oxford Instruments, Abingdon, UK), and the surface chemistry was studied using X-ray photoelectron spectroscopy (XPS, ESCALAB 250Xi, Thermo Fisher Scientific) with a monochromated Al Kα X-ray source (hα = 1486.6 eV). To assess the wetting properties of the prepared samples, the contact angles were measured by using a droplet shape analyzer (SmartDrop, Femtobiomed, Seongnam, Republic of Korea). The contact angles, which were measured five times at different locations on the surfaces, were used to calculate the mean values. The assessment of the adhesion strength at the interface between the AlN layer and its substrate was performed utilizing a microscratch testing apparatus (MST^3, Anton Paar, Graz, Austria). A conical Rockwell diamond indenter with a radius of 10 μm was used to apply a progressively augmenting load from 5 to 500 mN. This process was carried out at a constant speed of mm min^{-1}, resulting in a final sliding length of 3 mm. Notably, the scratch test was conducted on AlN anchored to a stainless-steel

https://doi.org/10.1021/acsomega.3c05524
ACS Omega 2023, 8, 42732−42740

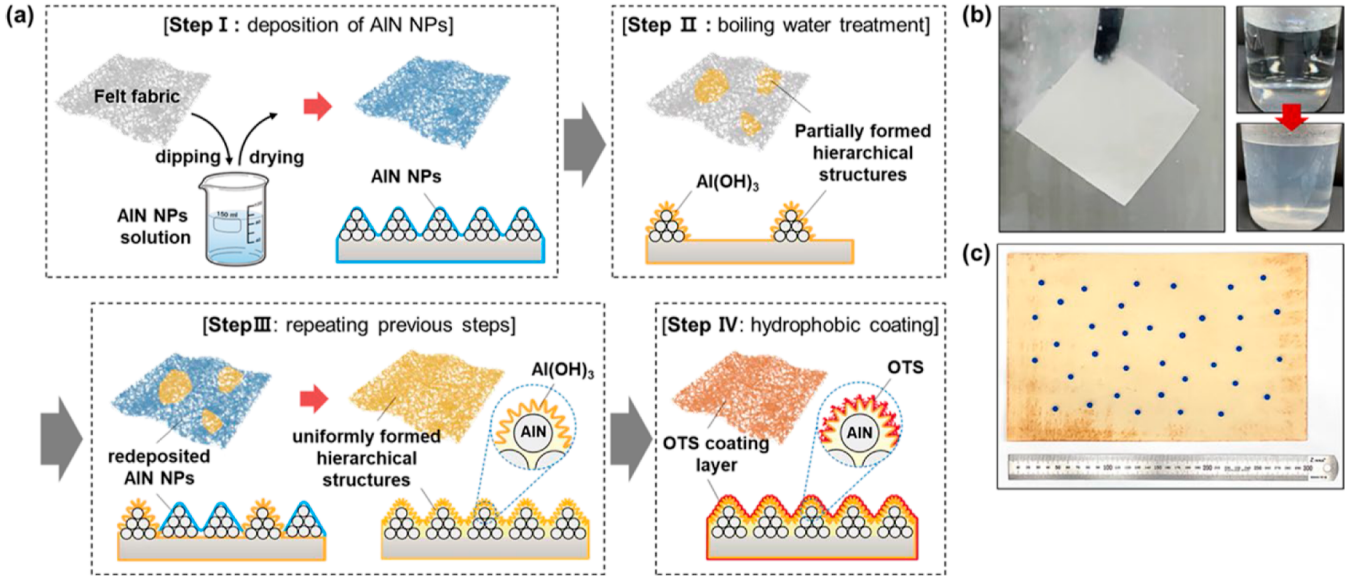

Figure 1. (a) Schematic diagram of the fabrication of the superhydrophobic−superoleophilic felt fabric. (b) Detachment of AlN nanoparticles and suspension of those detached particles in boiling water during hydrolysis. (c) Image of water droplets dyed with blue ink for visualization on the superhydrophobic felt fabric (size: 30 × 20 cm).

substrate, as measuring the adhesion strength was challenging owing to the porosity of the fiber. The scratches on the samples were observed by microscopic examination, and the critical load was defined as the load applied at the instance where the initial scratch was identified on the sample surface. An adhesive tape test was adopted to investigate the adhesion durability of the AlN layer to the felt fabric by using a standard test-grade tape (SP3020, TQC Sheen; adhesion strength of 7.6 N cm^{-1}).

2.4. Separation of Oil and Water. To evaluate the separation of immiscible water and oil, baskets were fabricated using the superhydrophobically treated fabric, and untreated cotton was placed inside. The baskets were then immersed in an oil/water mixture to evaluate the separation performance by quantifying the amount of oil absorbed by the superhydrophobic-treated cloth and untreated cotton relative to their initial masses. Diesel, gasoline, soybean oil, and *n*-hexane were used to evaluate the separation performance. The oil absorption performance was measured at room temperature, and the fabrics and cotton were rapidly weighed after removal from the solution to prevent the evaporation of the absorbed oil or organic solvent. Each experiment was repeated three times, and an average value was obtained. To evaluate the reusability of the superhydrophobic fabric, the absorbed oil was removed via simple mechanical squeezing. The fabric was placed in an oven at 65 °C for 3 h to evaporate the remaining solvent, the oil was subsequently reabsorbed, and the change in mass was measured. In addition, a 15 × 15 cm piece of modified felt fabric was mounted on a perforated plate to demonstrate the emulsion separation performance. An oil-and-water emulsion was prepared by using the ultrasonic homogenizer (100 W, 30 min) after mixing diesel and water in a ratio of 1:200 (v/v). After pressure was applied to the plate, the liquid passing through the superhydrophobic fabric was observed by using an optical microscope to determine whether the emulsion was separated.

3. RESULTS AND DISCUSSION

Superhydrophobic−superoleophilic felt fabric surfaces were fabricated based on the simple dip-coating deposition and hydrolysis of AlN nanopowder, as schematically shown in Figure 1a. A clean felt fabric is dipped into an ethanol solution containing the dispersed AlN nanopowder and then carefully removed from the solution. After the solution was removed by drying in an oven, a nanopowder film is deposited on the fabric surface (step I). The fabric is then immersed in boiling water, which hydrolyzes the AlN, converting it to $Al(OH)_3$ with a lamellar nanostructure. Consequently, a hierarchical surface morphology with micro- and nanoscale roughness develops on the fabric surface (step II). However, in simple dip-coating deposition, electrostatic and van der Waals interactions are the primary forces that generate adhesion between the particles and between the particles and fabric surface.[26−28] As the AlN particles are attached to the fabric via weak electrostatic forces, the surface tension forces cause most of the AlN particles to detach from the fabric surface during immersion in boiling water for hydrolysis. The particle loss is exacerbated by the bubbles generated in boiling water, and the number of detached particles increases with an increase in immersion rate. Particle loss may be reduced to a certain extent by decreasing the immersion rate, but it may not be completely eliminated. In addition, the detached particles may not redeposit on the surface of the fabric, which results in uneven attachment of the nanoparticles to the fabric surface (Figure 1b). To solve this problem, step I and step II were repeated several times to ensure that AlN nanoparticles with micro- and nanoscale roughness are evenly formed on the fabric surface (step III). After hydrophobic modification using alkylsilane materials, such as OTS, strong, stable covalent bonds are formed with $Al(OH)_3$ with no changes in the surface morphology.[29] With the formation of the hierarchical structures and hydrophobic coating layers, a durable superhydrophobic surface with exceptionally high contact and low sliding angles is successfully fabricated (step IV). These findings suggest the viability of preparing a superhydrophobic

https://doi.org/10.1021/acsomega.3c05524
ACS Omega 2023, 8, 42732−42740

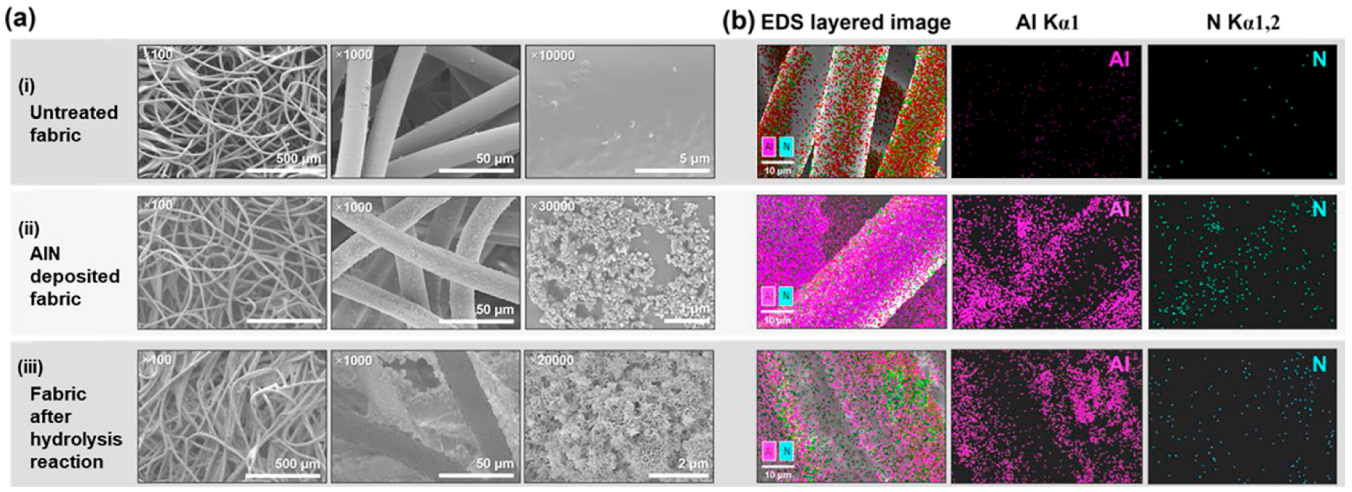

Figure 2. (a) SEM and (b) EDS mapping images of the fabric samples.

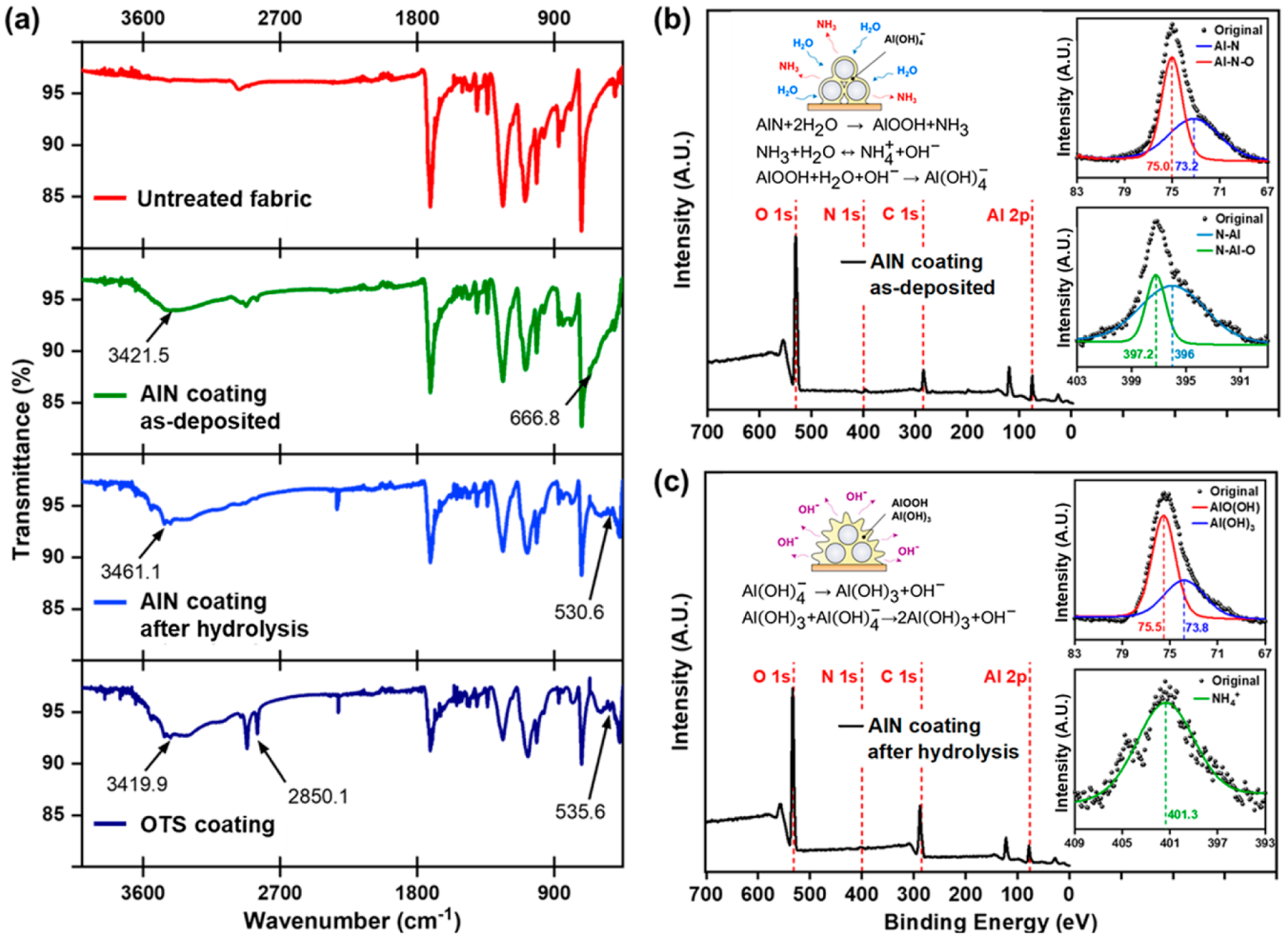

Figure 3. (a) ATR−FTIR spectra results related to the fabrication of the superhydrophobic−superoleophilic felt fabric. High-resolution XPS spectra of AlN before (b) and after (c) hydrolysis. The inset schematic diagrams shows morphological development during AlN hydrolysis and the chemical reactions involved.

surface, regardless of the size of the fabric, via the firm attachment of AlN nanoparticles to form a hierarchical structure without using an epoxy resin (Figure 1c).

To analyze the changes in the surface structure and chemical composition during hydrolysis, the AlN nanoparticles deposited on the felt fabric were examined by using SEM and EDS (Figure 2a,b). The original fabric surface, as shown in Figure 2a-i, is smooth, and no micro- or nanostructures that may increase the surface roughness are observed. Figure 2a-ii shows the surface with nanoparticles after dip-coating and spraying with the fixative, where the nanoparticles are uniformly attached to the fabric fibers. Upon immersion of

https://doi.org/10.1021/acsomega.3c05524
ACS Omega 2023, 8, 42732−42740

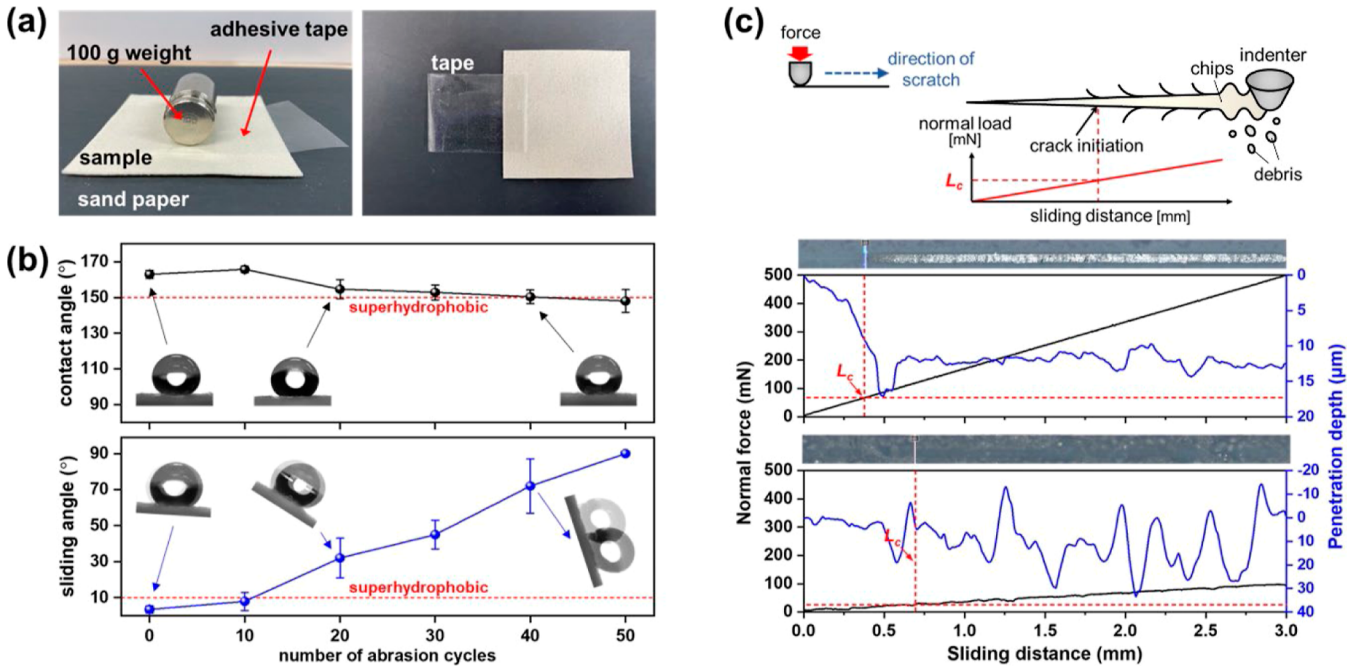

Figure 4. (a) Images of the tape-peeling test of the as-prepared superhydrophobic fabric. (b) Water contact and sliding angles as functions of the number of abrasion cycles. (c) Schematic diagram of the scratch test and the results observed via optical microscopy corresponding to the initial surface failures of the AlN- (top) and NeverWet-coated (bottom) substrates.

the fabric in boiling water, AlN is converted to $Al(OH)_3$ with a lamellar nanostructure, resulting in the formation of a hierarchical surface structure encompassing micro- and nanoscale features (Figure 2a-iii). EDS reveals that the nanoparticle-deposited surface exhibits even distinct distributions of Al and N, which are the primary components of AlN, compared to those of the bare fabric surface. The faint change in contrast corresponding to N after hydrolysis may be attributed to the formation of a layer of $Al(OH)_3$ on the AlN surface, which leads to changes in the chemical composition.

ATR-FTIR analysis was used to study specific changes in the chemical composition during the surface modification of the fabrics. As shown in Figure 3a, a distinct absorbance increase at 668 cm^{-1} was observed after AlN nanopowder attachment, which corresponds to the absorption peak of the Al−N stretching vibration.[30] Also, broad and smooth absorption bands in the 450−900 and 3300−3700 cm^{-1} ranges are associated with Al−O and O−H stretching vibrations, respectively.[31] As shown in Figure 3c, a band at 530.6 cm^{-1} associated with the stretching mode of Al−O and a band at 3461.1 cm^{-1} associated with the characteristic stretching vibration of O−H are clearly observed. These spectra show evidence of the conversion of AlN to aluminum hydroxide due to the following hydrolysis reaction[32]

$$AlN + 2H_2O \rightarrow AlOOH + NH_3$$

On the other hand, a strong peak at 2850 cm^{-1} was observed after the OTS coating, which was attributed to the C−H stretching of the methyl group. This is because OTS has a hydrophobic methyl group ($-CH_3$) as a functional group, and it can be inferred that the OTS layer was successfully formed on the hydrated AlN.[33] In addition, XPS was employed to explore in depth the alterations in the chemical composition before and after AlN hydrolysis. Figure 3b,c shows the high-resolution XP spectra and their corresponding fitted curves of the Al 2p and N 1s peaks from the AlN film deposits. As shown in Figure 3b, the Al 2p and N 1s peaks are each deconvoluted into two peaks, mainly corresponding bonds: Al−N (73.2 and 396 eV) and Al−N−O (75.0 and 397.2 eV).[34,35] The latter bond, commonly identified as aluminum oxynitride (AlO_xN_y),[27] implies the existence of a passivation layer due to reaction with the atmosphere when the nanoparticles are exposed to air. After hydrolysis, the Al 2p peak splits into subpeaks at 75.5 and 73.8 eV, whereas the N 1s peak shows a main contribution at about 401.3 eV (Figure 3c) due to the hydrolysis producing AlOOH and NH_3. Notably, the 73.8 eV subpeak in the Al 2p spectrum aligns with $Al(OH)_3$, suggesting further chemical reactions involving an increase in pH by the production of NH_3. This mildly alkaline solution leads to the formation of a gelatinousaluminate ion intermediate ($Al(OH)_4^-$) from AlOOH.[36,37] The formation of a thin film of aluminate gel on the surfaces of the AlN particles aids in filling the interparticle spaces and generates adhesion at particle-to-particle and particle-to-substrate. The bonding between the particles and substrate occurs via a combination of hydrogen and covalent bonding to the substrate OH groups (inset image of Figure 3b).[38] The process involves the subsequent crystallization of the aluminate gel layer into $Al(OH)_3$, accompanied by polymerization and nanostructure formation, augmenting surface roughness and mechanical robustness (inset image of Figure 3c).[39] Therefore, higher levels of surface roughness and mechanical robustness may be realized via the formation of surface structures. When a sample is placed in boiling water to induce hydrolysis, bubbles and surface tension may lead to detachment of the nanoparticles from the fiber surface. To prevent this, an epoxy resin may be used to attach the nanoparticles to the surface, but this may inhibit the reaction between AlN and water, thereby hindering hydration and morphological evolution. Thus, the hydrolysis reaction of AlN allows the firmly attaching of nanoparticles to a material surface without using an epoxy resin and generating a hierarchical structure that enables surface superhydrophobicity.

https://doi.org/10.1021/acsomega.3c05524
ACS Omega 2023, 8, 42732−42740

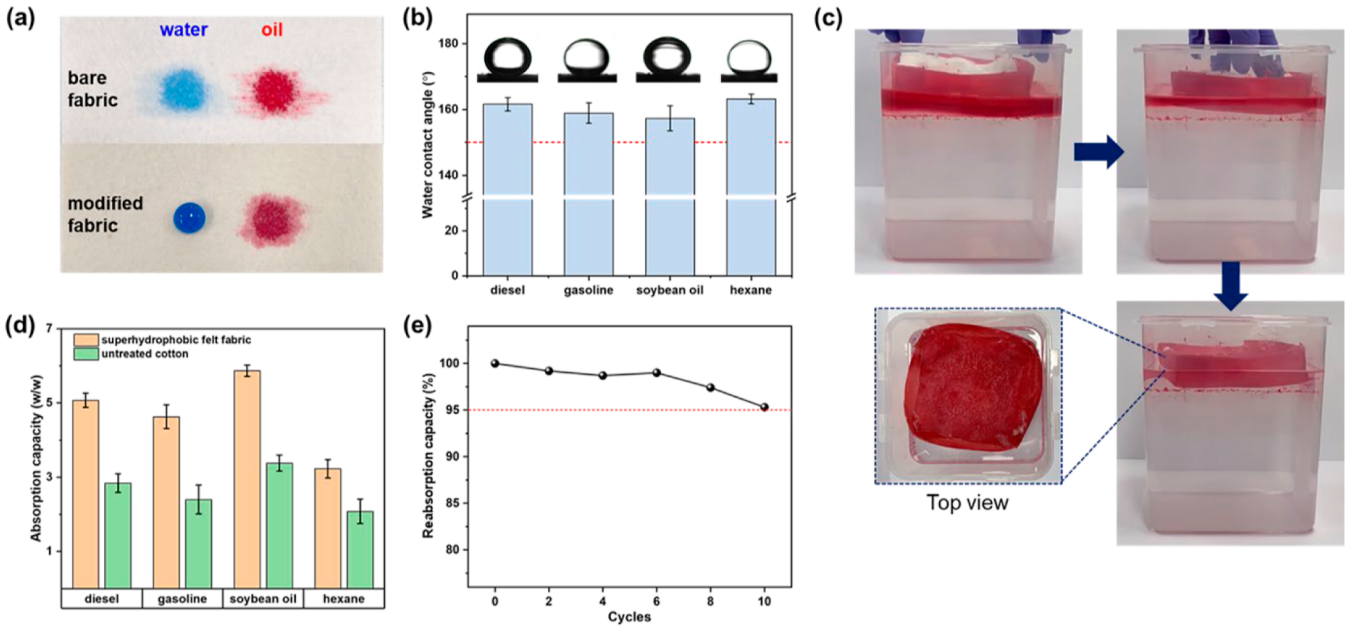

Figure 5. (a) Sample images showing the wetting properties of bare and modified fabric surface. (b) Water contact angles of the superhydrophobic fabric in different oils (diesel, gasoline, soybean oil, and hexane). (c) Images showing oil (diesel dyed with red O) removal via absorption from the water surface. (d) Absorption capacities of the superhydrophobic fabric and untreated cotton for various oils and organic solvents. (e) Reabsorption capacity of the superhydrophobic fabric over 10 cycles of absorption and drying.

The long-term mechanical durability of superhydrophobic coatings, particularly their abrasion resistances, is a critical factor that limits their practical applications. Figure 4a shows a tape-peeling test of an AlN-deposited superhydrophobic fabric sample. A 100 g mass is applied to firmly attach the tape, and the coating layer hardly detaches from the sample surface after the tape is removed. To evaluate the abrasion resistance of the AlN-deposited fabric surface, it was rubbed with sandpaper, and changes in the contact angle of the surface are observed as the number of rubbing cycles increased (Figure 4b). To account for the nanoparticle size, the abrasion resistance of the coating was evaluated using a back-and-forth motion under a load, with 2000# sandpaper placed under the fabric surface and a 100 g mass placed on top. The AlN-coated superhydrophobicfelt fabric exhibits excellent mechanical properties, with high contact and low sliding angles of >160 and <10°, respectively, even after 10 abrasion cycles. Although the sliding angle increases rapidly with the number of abrasion cycles, a high contact angle of >150° is still observed after 50 abrasion cycles. Furthermore, a scratch test was conducted to qualitatively estimate the interfacial adhesion between the deposited AlN film and substrate. To determine the critical load of the AlN film and its bond strength with the substrate, a conical diamond tip was moved across the surface of the film under an increasing load until a clear fracture occurs. The critical load was identified as the load at which the initial scratch occurred on the surface, and the surface fracture was evaluated using optical examination, as illustrated in Figure 4c. In addition, the bond strengths of the AlN layer and a commercially available superhydrophobic coating (NeverWet) were compared. Surfaces coated with NeverWet exhibit superhydrophobic characteristics as a result of functionalized silica nanoparticles with the tens of nanometers scale in conjunction with an epoxy resin used to anchor them to the base material. Once the first crack is observed on the AlN-deposited surface, the AlN particle layer undergoes interfacial failure, causing partial detachment of the layer and exposing the surface of the substrate. As scratching continues, the deposited layers become detached from the substrates and the substrate is completely exposed, which is defined as an adhesion failure at the coating/substrate interface. The adhesion strengths of the AlN layer and NeverWet are 65.3 and 26.0 mN, respectively. The superior adhesion strength of the AlN-bearing sample compared to that of the NeverWet-coated sample may be attributed to the self-bonding of the nanoparticles with $Al(OH)_3$. The NeverWet coating is composed of an adhesive layer on the bottom and a functionalized silica nanoparticle layer on the top,[40] and the low adhesion strength is likely due to the nanoparticles failing to bond with the adhesive layer on the bottom and adhering poorly to the coating layer on top. Furthermore, the presence of cracks in the top layer of the NeverWet coating could potentially weaken its robustness, resulting in significant alterations in the depth of penetration throughout the scratch test.

Materials with special wettabilities are crucial in the selective separation of water/oil mixtures, and the wettabilities of the bare and modified fabrics are shown in Figure 5a. The surface of the bare fabric was wetted using water and oil, with both liquids penetrating the fabric surface. Conversely, the modified fabric surface is superoleophilic and -hydrophobic, exhibiting complete wetting with oil and no wetting with water. Moreover, the under-oil contact angles were measured in various liquids, including diesel, gasoline, soybean oil, and hexane. High contact angles of >150° are observed (Figure 5b), owing to the hierarchical structure formed by the AlN nanoparticles on the fiber surface, in addition to the inherently low surface energy. These characteristics are highly desirable in developing an effective filter material that may selectively separate oil from oily wastewater. In this study, we attempted to separate immiscible mixtures of water and four different types of oils. The separation performance was evaluated by

https://doi.org/10.1021/acsomega.3c05524
ACS Omega 2023, 8, 42732−42740

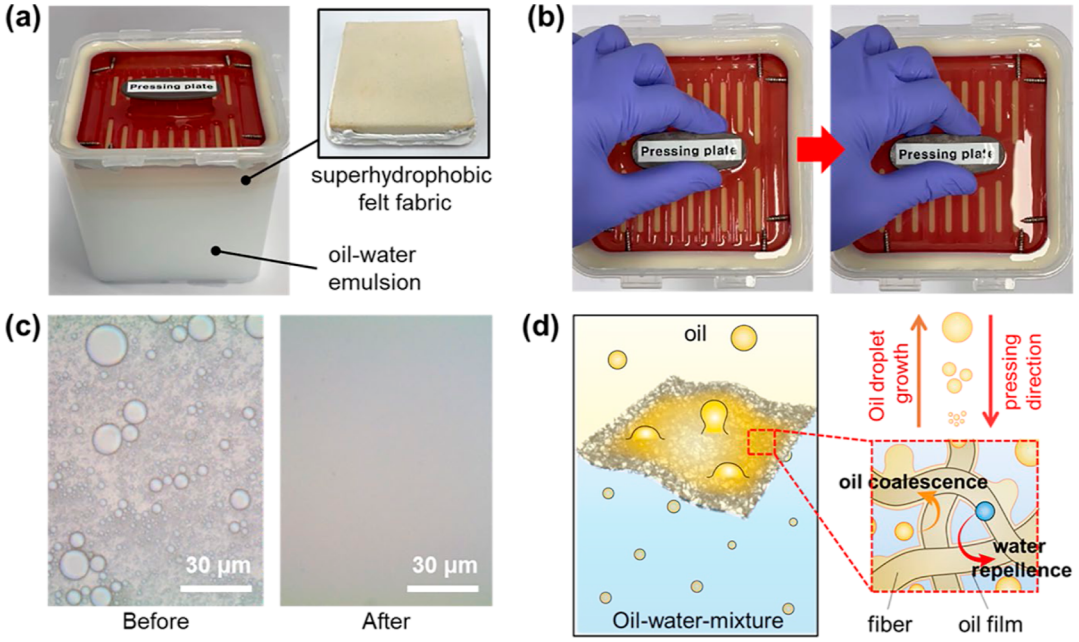

Figure 6. (a) Simple experimental setup of oil/water emulsion separation. (b) Images showing emulsion separation by pressing the plate with the as-prepared superhydrophobic felt fabric. (c) Optical images revealing the diesel-in-water emulsion separation performance. (d) Mechanism of emulsion separation through the superhydrophobic−superoleophilic felt fabric.

quantifying the amounts of oil absorbed by the modified fabric and untreated cotton relative to their initial masses (Figure 5c). The oil absorption capacities of the modified fabric and untreated cotton are shown in Figure 5d. Superhydrophobic treatment of the fabric results in exceptional oil absorption properties, with a capacity of over five times its original mass, except for that in hexane. In comparison, the untreated cotton absorbs approximately three times its mass in oil. The lowest absorption capacities are observed for hexane and gasoline. The reduced capacity for hexane is attributed to its high evaporation rate, which causes a significant portion of the absorbed gas to evaporate. The oil absorbed by the modified fabric was extracted, and the fabric was dried and reused to evaluate its absorbency (Figure 5e). In this paper, the reabsorption capacity of the felt fabric is defined to represent the change in the quantity of oil absorbed after multiple uses compared to its initial performance, assuming the initial oil absorption capacity is 100. Even after >10 reuse cycles, little difference in the absorbency is observed, which may be due to the excellent adhesion strength of AlN on the fiber surface. However, the slight decrease in reabsorption capacity with increasing reuse cycle might be attributed to oven drying for oil removal on the fabric during the reuse tests. The drying process could not effectively remove the oil bound to the surface structure, resulting in deterioration of the surface wetting behaviors and reduced separation performance of the fabric.

An efficient, cost-effective, green emulsion separation remains a significant challenge, and the modified fabric displays the potential to effectively separate emulsions in addition to its superior absorption capacity. The emulsion separation performance of the fabric surface is evaluated by fixing the fabric onto a perforated plate and placing it in a container, and the sides of the plate are sealed with silicone (Figure 6a). The emulsion droplets containing water droplets with sizes of several to tens of micrometers were observed under a light microscope prior to separation. Upon applying pressure to the plate, the milky emulsion passes through the fabric, and the clear oil is separated successfully (Figure 6b). No water droplets are present in the separated oil, as confirmed via microscopy (Figure 6c). To elucidate the separation mechanism of the water-in-oil emulsion utilizing the modified fabric more thoroughly, a schematic representation of the separation procedure is depicted in Figure 6d. Due to its superhydrophobic/-oleophilic properties, the fabric repels water while allowing tiny oil droplets to pass through continuously. Tangled weblike fiber structures within the fabric may trap small oil droplets and promote their coalescence into larger droplets on the fiber surfaces. According to Stokes' law, larger oil droplets float faster, and thus, the formation of large oil droplets may facilitate demulsification and separation.[18] Therefore, oil droplets smaller than the pore size may be separated.

4. CONCLUSIONS

This study presented a facile approach for use in preparing superhydrophobic fabric materials via self-adhesion and morphological evolution based on the hydrolysis of AlN nanopowders. This method involved temporary immobilization of AlN nanopowders on the fabric surfaces using a water-soluble fixative, which improved the weak adhesion between the nanopowders and fabrics, while ensuring that the formation of the surface structures during hydration was unaffected. This enabled the formation of surface structures with excellent adhesion to the fabric without requiring the addition of a binder resin. The resulting fabric exhibited a high porosity and superhydrophobic structure, which endowed it with excellent absorption capacities for various oils, and furthermore, oils could be separated from emulsions with high efficiencies. This method is green and cost-effective, as it does not require the use of strong acids or bases. Additionally, the solution preparation and surface coating processes are straightforward, which substantially reduces the potential environmental hazard

https://doi.org/10.1021/acsomega.3c05524
ACS Omega 2023, 8, 42732−42740

and markedly decreases the cost of application. Thus, the superhydrophobic fabric developed in this study exhibits considerable potential for use in treating oil pollution including oil spill cleanup, fuel refinement, and emulsion separation.

AUTHOR INFORMATION

Corresponding Author

Handong Cho − *Department of Mechanical Engineering, Mokpo National University, Muan, Jeonnam 58554, Republic of Korea;* orcid.org/0000-0002-7169-8325; Email: hdcho@mnu.ac.kr

Authors

Jihoon Chung − *Department of Mechanical Design Engineering, Kumoh National Institute of Technology, Gumi-si, Gyeongsangbuk-do 39177, Republic of Korea*

Sangmin Lee − *School of Mechanical Engineering, Chung-Ang University, Seoul 06974, Republic of Korea*

Complete contact information is available at: https://pubs.acs.org/10.1021/acsomega.3c05524

Notes

The authors declare no competing financial interest.

ACKNOWLEDGMENTS

This research was supported by Research Funds of Mokpo National University in 2020.

REFERENCES

(1) Beyer, J.; Trannum, H. C.; Bakke, T.; Hodson, P. V.; Collier, T. K. Environmental Effects of the Deepwater Horizon Oil Spill: A Review. *Mar. Pollut. Bull.* **2016**, *110* (1), 28−51.

(2) Ge, J.; Zhao, H.; Zhu, H.; Huang, J.; Shi, L.; Yu, S. Advanced Sorbents for Oil-Spill Cleanup: Recent Advances and Future Perspectives. *Adv. Mater.* **2016**, *28* (47), 10459−10490.

(3) Kavalenka, M. N.; Vüllers, F.; Kumberg, J.; Zeiger, C.; Trouillet, V.; Stein, S.; Ava, T. T.; Li, C.; Worgull, M.; Hölscher, H. Adaptable Bioinspired Special Wetting Surface for Multifunctional Oil/Water Separation. *Sci. Rep.* **2017**, *7* (1), 39970.

(4) Liu, S.; Zhang, Q.; Fan, L.; Wang, R.; Yang, M.; Zhou, Y. 3D Superhydrophobic Sponge Coated with Magnesium Hydroxide for Effective Oil/Water Mixture and Emulsion Separation. *Ind. Eng. Chem. Res.* **2020**, *59* (25), 11713−11722.

(5) Zhang, W.; Liu, N.; Cao, Y.; Lin, X.; Liu, Y.; Feng, L. Superwetting Porous Materials for Wastewater Treatment: From Immiscible Oil/Water Mixture to Emulsion Separation. *Adv. Mater. Interfaces* **2017**, *4* (10), 1600029.

(6) Saththasivam, J.; Loganathan, K.; Sarp, S. An Overview of Oil-Water Separation Using Gas Flotation Systems. *Chemosphere* **2016**, *144*, 671−680.

(7) Klasson, K. T.; Taylor, P. A.; Walker, J. F.; Jones, S. A.; Cummins, R. L.; Richardson, S. A. Modification of a Centrifugal Separator for In-Well Oil-Water Separation. *Sep. Sci. Technol.* **2005**, *40* (1−3), 453−462.

(8) Santos, A. S.; Oliveira, L. F. S.; Marques, A. M.; Silva, D. C.; Mansur, C. R. Evaluation of the Efficiency of Polyethylenimine as Flocculants in the Removal of Oil Present in Produced Water. *Colloids Surf., A* **2018**, *558*, 200−210.

(9) Saththasivam, J.; Ogunbiyi, O.; Lawler, J.; Al-Rewaily, R.; Liu, Z. Evaluating Dissolved Air Flotation for Oil/Water Separation Using a Hybridized Coagulant of Ferric Chloride and Chitosan. *J. Water Process Eng.* **2022**, *47*, 102836.

(10) Alabresm, A.; Chen, Y. P.; Decho, A. W.; Lead, J. A Novel Method for the Synergistic Remediation of Oil-Water Mixtures Using Nanoparticles and Oil-Degrading Bacteria. *Sci. Total Environ.* **2018**, *630*, 1292−1297.

(11) Okoro, V.; Azimov, U.; Munoz, J.; Hernandez, H. H.; Phan, A. N. Microalgae Cultivation and Harvesting: Growth Performance and Use of Flocculants - A Review. *Renew. Sustain. Energy Rev.* **2019**, *115*, 109364.

(12) Wang, J.; Liu, S. Fabrication of Water-Repellent Double-Layered Polydopamine/Copper Films on Mesh with Improved Abrasion and Corrosion Resistance by Solution-Phase Reduction for Oily Wastewater Treatment. *Sep. Purif. Technol.* **2020**, *233*, 116005.

(13) Deng, Y.; Wu, Y.; Chen, G.; Zheng, X.; Dai, M.; Peng, C. Metal-Organic Framework Membranes: Recent Development in the Synthesis Strategies and Their Application in Oil-Water Separation. *Chem. Eng. J.* **2021**, *405*, 127004.

(14) Kim, S.; Cho, H.; Hwang, W. Robust Superhydrophilic Depth Filter and Oil/Water Separation Device with Pressure Control System for Continuous Oily Water Treatment on a Large Scale. *Sep. Purif. Technol.* **2021**, *256*, 117779.

(15) Hao, W.; Xu, J.; Li, R.; Zhao, X.; Qiu, L.; Yang, W. Developing Superhydrophobic Rock Wool for High-Viscosity Oil/Water Separation. *Chem. Eng. J.* **2019**, *368*, 837−846.

(16) Rasouli, S.; Rezaei, N.; Hamedi, H.; Zendehboudi, S.; Duan, X. Superhydrophobic and Superoleophilic Membranes for Oil-Water Separation Application: A Comprehensive Review. *Mater. Des.* **2021**, *204*, 109599.

(17) Li, K.; Ju, J.; Xue, Z.; Ma, J.; Feng, L.; Gao, S.; Jiang, L. Structured Cone Arrays for Continuous and Effective Collection of Micron-Sized Oil Droplets from Water. *Nat. Commun.* **2013**, *4* (1), 2276.

(18) Woo, S.; Cho, H.; Park, J.; Shin, Y.; Hwang, W. A Novel Approach to Designing a Biomimetic Wettable Patterned Surface for Highly Efficient and Continuous Surfactant-Free Oil Emulsion Separation. *Sep. Purif. Technol.* **2020**, *248*, 116864.

(19) Ma, W.; Zhao, J.; Oderinde, O.; Han, J.; Liu, Z.; Gao, B.; Xiong, R.; Zhang, Q.; Jiang, S.; Huang, C. Durable Superhydrophobic and Superoleophilic Electrospun Nanofibrous Membrane for Oil-Water Emulsion Separation. *J. Colloid Interface Sci.* **2018**, *532*, 12−23.

(20) Qing, W.; Shi, X.; Deng, Y.; Zhang, W.; Wang, J.; Tang, C. Y. Robust Superhydrophobic-Superoleophilic Polytetrafluoroethylene Nanofibrous Membrane for Oil/Water Separation. *J. Membr. Sci.* **2017**, *540*, 354−361.

(21) Cho, H.; Lee, J.; Lee, S.; Hwang, W. Durable Superhydrophilic/Phobic Surfaces Based on Green Patina with Corrosion Resistance. *Phys. Chem. Chem. Phys.* **2015**, *17* (10), 6786−6793.

(22) Yang, X. Y.; Chen, L. H.; Li, Y.; Rooke, J. C.; Sanchez, C.; Su, B. L. Hierarchically Porous Materials: Synthesis Strategies and Structure Design. *Chem. Soc. Rev.* **2017**, *46* (2), 481−558.

(23) Ge, M.; Cao, C.; Huang, J.; Zhang, X.; Tang, Y.; Zhou, X.; Zhang, K.; Chen, Z.; Lai, Y. Rational Design of Materials Interface at Nanoscale towards Intelligent Oil-Water Separation. *Nanoscale Horiz.* **2018**, *3* (3), 235−260.

(24) Zhang, J.; Li, B.; Wu, L.; Wang, A. Facile Preparation of Durable and Robust Superhydrophobic Textiles by Dip Coating in Nanocomposite Solution of Organosilanes. *Chem. Commun.* **2013**, *49* (98), 11509−11511.

(25) Ge, D.; Yang, L.; Wu, G.; Yang, S. Spray Coating of Superhydrophobic and Angle-Independent Coloured Films. *Chem. Commun.* **2014**, *50* (19), 2469−2472.

(26) Sarkar, P.; De, D.; Uchikochi, T.; Besra, L. Electrophoretic Deposition (EPD): Fundamentals and Novel Applications in Fabrication of Advanced Ceramic Microstructures. In *Electrophoretic Deposition of Nanomaterials*; Dickerson, J. H., Boccaccini, A. R., Eds.; Nanostructure Science and Technology; Springer: New York, NY, 2012, pp 181−215.

(27) Ammam, M. Electrophoretic Deposition under Modulated Electric Fields: A Review. *RSC Adv.* **2012**, *2* (20), 7633−7646.

(28) Lee, K.; Hwang, W.; Cho, H. Development of a Versatile Coating Based on Hydrolysis-Assisted Self-Bonding and Structure Evolution of Aluminum Nitride Nanopowder: Application toward Repairing Severe Damages on Superhydrophobic Surfaces. *Surf. Coat. Technol.* **2023**, *460*, 129431.

(29) Cho, H.; Jeong, J.; Kim, W.; Choi, D.; Lee, S.; Hwang, W. Conformable Superoleophobic Surfaces with Multi-Scale Structures on Polymer Substrates. *J. Mater. Chem. A* **2016**, *4* (21), 8272−8282.
(30) Cano, A. M.; Lii-Rosales, A.; George, S. M. Thermal Atomic Layer Etching of Aluminum Nitride Using HF or XeF2 for Fluorination and BCl3 for Ligand Exchange. *J. Phys. Chem. C* **2022**, *126* (16), 6990−6999.
(31) Du, X.; Wang, Y.; Su, X.; Li, J. Influences of PH Value on the Microstructure and Phase Transformation of Aluminum Hydroxide. *Powder Technol.* **2009**, *192* (1), 40−46.
(32) Barroso, M. N.; Gomez, M. F.; Arrúa, L. A.; Abello, M. C. Reactivity of Aluminum Spinels in the Ethanol Steam Reforming Reaction. *Catal. Lett.* **2006**, *109* (1−2), 13−19.
(33) Kamaraj, R.; Vasudevan, S. Facile One-Pot Electrosynthesis of Al(OH)3 - Kinetics and Equilibrium Modeling for Adsorption of 2,4,5-Trichlorophenoxyacetic Acid from Aqueous Solution. *New J. Chem.* **2016**, *40* (3), 2249−2258.
(34) Zhang, J.; Zhang, Q.; Yang, H.; Wu, H.; Zhou, J.; Hu, L. Bipolar Resistive Switching Properties of AlN Films Deposited by Plasma-Enhanced Atomic Layer Deposition. *Appl. Surf. Sci.* **2014**, *315*, 110−115.
(35) Rosenberger, L.; Baird, R.; McCullen, E.; Auner, G.; Shreve, G. XPS Analysis of Aluminum Nitride Films Deposited by Plasma Source Molecular Beam Epitaxy. *Surf. Interface Anal.* **2008**, *40* (9), 1254−1261.
(36) Cho, H.; Kim, D.; Lee, C.; Hwang, W. A Simple Fabrication Method for Mechanically Robust Superhydrophobic Surface by Hierarchical Aluminum Hydroxide Structures. *Curr. Appl. Phys.* **2013**, *13* (4), 762−767.
(37) Cho, H.; Park, B.; Kim, M.; Lee, S.; Hwang, W. A Large-Scale Water-Harvesting Device with β-Al(OH)3 Microcone Arrays by Simple Hydrothermal Synthesis. *J. Mater. Chem. A* **2017**, *5* (48), 25328−25337.
(38) Tiringer, U.; van Dam, J.; Abrahami, S.; Terryn, H.; Kovač, J.; Milošev, I.; Mol, J.; J, M. C. M. Scrutinizing the Importance of Surface Chemistry versus Surface Roughness for Aluminium/Sol-Gel Film Adhesion. *Surf. Interfaces* **2021**, *26*, 101417.
(39) Bye, G. C.; Robinson, J. G. Crystallization Processes in Aluminium Hydroxide Gels. *Kolloid Z. Z. Polym.* **1964**, *198* (1−2), 53−60.
(40) Li, C.; Boban, M.; Beebe, J. M.; Bhagwagar, D. E.; Liu, J.; Tuteja, A. Non-Fluorinated, Superhydrophobic Binder-Filler Coatings on Smooth Surfaces: Controlled Phase Separation of Particles to Enhance Mechanical Durability. *Langmuir* **2021**, *37* (10), 3104−3112.

https://doi.org/10.1021/acsomega.3c05524
ACS Omega 2023, 8, 42732−42740